- 9-10 August 2024. RIKEN, Japan

- International Workshop on Quark Structure of Hadrons 2024

Two-pion emission decays of negative parity singly heavy baryons

Nongnapat Ponkhuha[1]
Ahmad Jafar Arifi[2], Daris Samart[1]

[1]Department of Physics, Faculty of Science, Khon Kaen University, Khon Kaen 40002, Thailand.
[2]Few-body Systems in Physics Laboratory, RIKEN Nishina Center, Wako 351-0198, Japan.

Table of contents

Two-pion emission decays of negative parity singly heavy baryons

Introduction

Heavy baryons

- Heavy baryons are particles composed of **one heavy quark** (charm or bottom) and **two light quarks** (up, down, or strange).

- Provide insights into the interplay between light-quark dynamics and heavy-quark symmetry (HQS)

- The dynamics of light quarks are governed by chiral symmetry.

- In the heavy-quark limit, the spin of heavy quarks decouples from these dynamics, which are then governed by heavy-quark symmetry (HQS)

- This interplay of symmetries plays a crucial role in understanding the structure of heavy baryons. heavy baryons exhibit a separation between orbital motions, such as $\lambda-$ mode $(l_\lambda \neq 0)$ and $\rho-$mode $(l_\rho \neq 0)$, and have relatively smaller widths that facilitate their analysis.

- The light quarks can form antisymmetric $(s = 0)$or symmetric $(s = 1)$ spin configurations, with orbital excitations in the λ or ρ mode.

- The low-lying singly heavy baryons are expected to be dominated by the $\lambda-$mode excitations

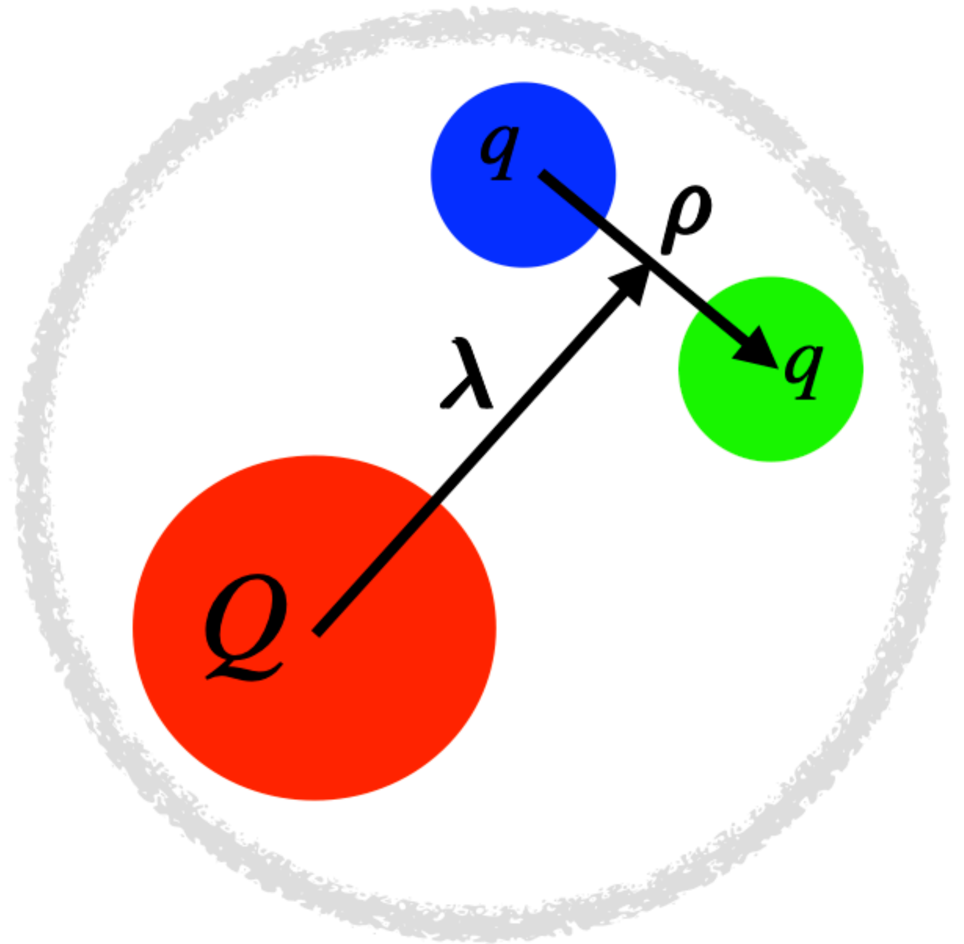

Background of study

- Specifically, the strong decays of excited singly heavy baryons, especially through two-pion emission processes.

- Most Λ_Q and Ξ_Q particles with $Q = c, b$ are observed in this decay mode.

- In addition to total decay width or branching ratio, three-body decays contain more complex structures.

- These structures are evident in the Dalitz plots and invariant mass distributions, providing additional constraints on the structures of heavy baryons.

- In our analysis, we will show that is invariant mass distribution depends on the spin-parity, (J^P), assignment which may suggest that they are possible radial excited states by using non-relativistic quark model.

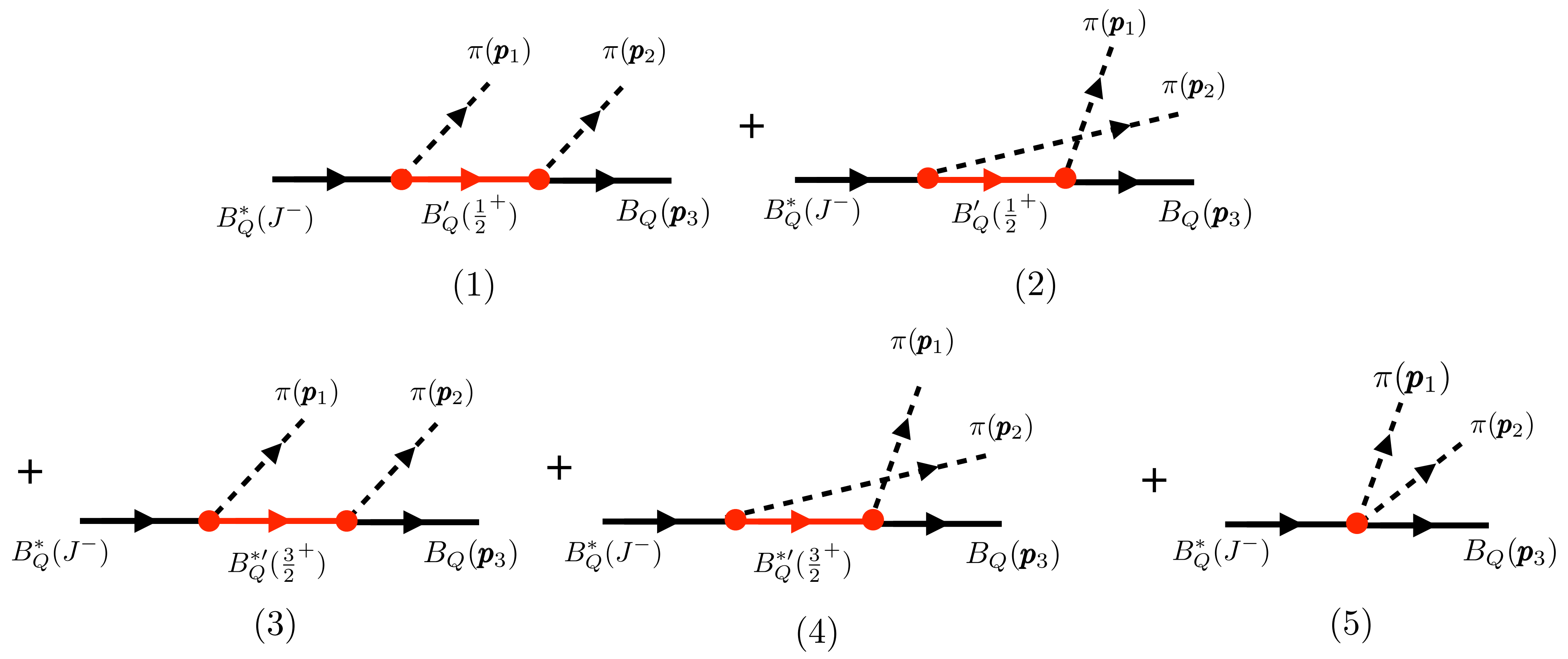

Objective

Two-pion emission decays of negative parity singly heavy baryons

- Our primary objective is to investigate the decay processes of these baryons, specifically looking at both sequential and direct processes.
- We aim to compare our theoretical predictions with experimental data, particularly those from the Belle experiment.

Methodology

Three-body decays

- The decays we analyzed occur through sequential processes involving intermediate states from the symmetric flavor sextet or direct processes.
- Sequential processes are crucial for understanding the contributions of intermediate states.
- The direct process is vital for comparing our theoretical predictions with experimental data.

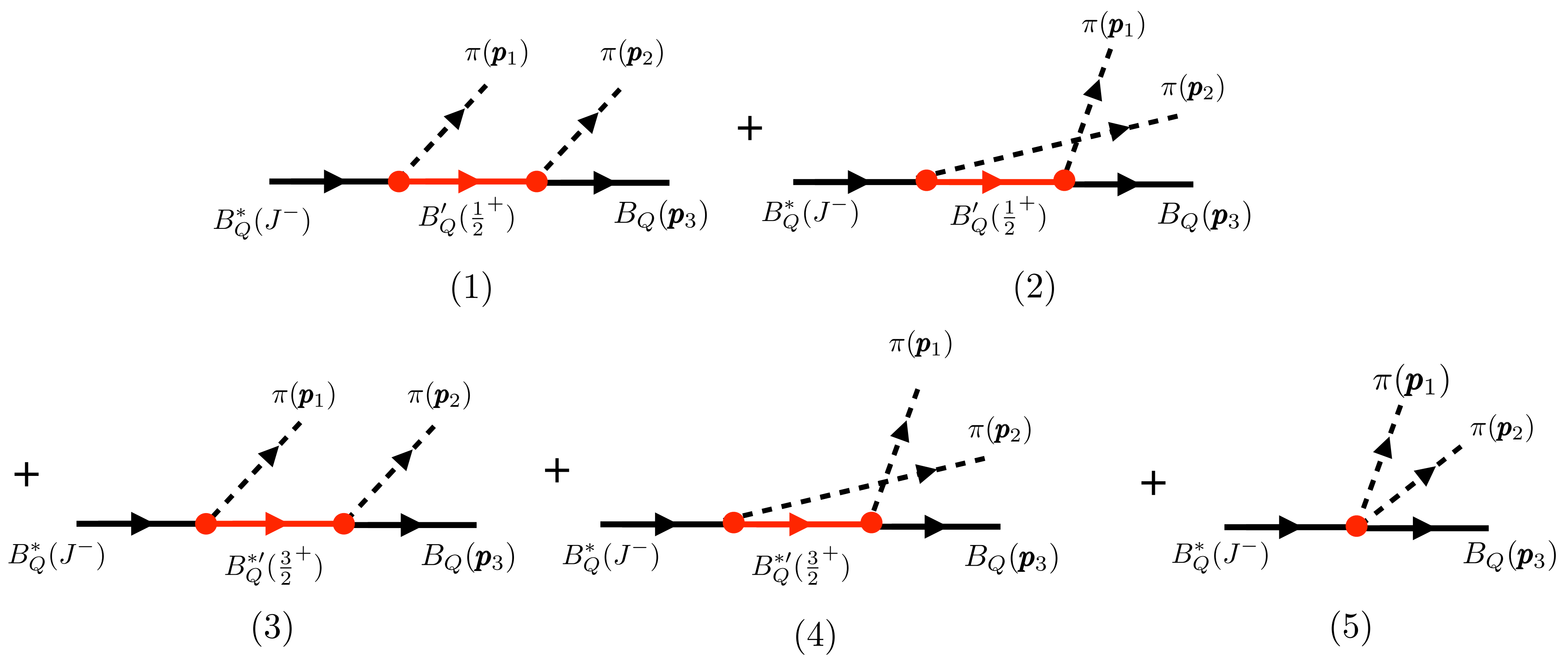

Fig.1 Two-pion emission decays of heavy baryons $B_Q^*(J^-)$ where

$$\mathscr{M}_1 = \frac{g_{11}^{a} g_{11}^{b} N \chi^\dagger_{B_Q\left(\frac{1}{2}^+\right)} \left(\boldsymbol{\sigma}\cdot\boldsymbol{p}_2\right) \chi_{B_Q^*\left(\frac{1}{2}^-\right)}}{m_{\pi_2 B_Q} - m_{B_Q'\left(\frac{1}{2}+\right)} + \frac{i}{2}\Gamma_{B_Q'\left(\frac{1}{2}^+\right)}} \quad (1)$$

$$\mathscr{M}_2 = \frac{g_{13}^{a} g_{31}^{b} N \chi^\dagger_{B_Q\left(\frac{1}{2}^+\right)} \left(\boldsymbol{S}\cdot\boldsymbol{p}_2\right)\left(\boldsymbol{S}^\dagger\cdot\boldsymbol{p}_1\right)\left(\boldsymbol{\sigma}\cdot\boldsymbol{p}_1\right) \chi_{B_Q^*\left(\frac{1}{2}^-\right)}}{m_{\pi_2 B_Q} - m_{B_Q'\left(\frac{3}{2}^+\right)} + \frac{i}{2}\Gamma_{B_Q'\left(\frac{3}{2}^+\right)}} \quad (2)$$

$$\mathscr{M}_3 = \frac{g_{11}^{a'} g_{11}^{b'} N \chi^\dagger_{B_Q\left(\frac{1}{2}^+\right)} \left(\boldsymbol{\sigma}\cdot\boldsymbol{p}_1\right) \chi_{B_Q^*\left(\frac{1}{2}^-\right)}}{m_{\pi_1 B_Q} - m_{B_Q'\left(\frac{1}{2}^+\right)} + \frac{i}{2}\Gamma_{B_Q'\left(\frac{1}{2}^+\right)}} \quad (3)$$

$$\mathscr{M}_4 = \frac{g_{13}^{a'} g_{31}^{b'} N \chi^\dagger_{B_Q\left(\frac{1}{2}^+\right)} \left(\boldsymbol{S}\cdot\boldsymbol{p}_1\right)\left(\boldsymbol{S}^\dagger\cdot\boldsymbol{p}_2\right)\left(\boldsymbol{\sigma}\cdot\boldsymbol{p}_2\right) \chi_{B_Q^*\left(\frac{1}{2}^-\right)}}{m_{\pi_2 B_Q} - m_{B_Q'\left(\frac{3}{2}^+\right)} + \frac{i}{2}\Gamma_{B_Q'\left(\frac{3}{2}^+\right)}} \quad (4)$$

$$\mathscr{M}_5 = \frac{g_{11}^{d} N}{f_\pi} \chi^\dagger_{B_Q} (\boldsymbol{\sigma}\cdot(\boldsymbol{p}_1 + \boldsymbol{p}_2)) \chi_{B_Q^*} \quad (5)$$

- The $\tilde{B}_Q^{(\prime)}$ and $\tilde{B}_Q^{*(\prime)}$ are the intermediate states belonging to the symmetric flavor sextet 6_F of heavy baryon, and their mass distribution is modeled by a Breit-Wigner function.
-

Three-body decays

- In general, due to the $S-$wave nature decay of the first vertex, it is expected that processes $\mathscr{M}_1(\tilde{B}_Q)$ and $\mathscr{M}_3(\tilde{B}'_Q)$ will dominate over processes $B^*_Q(1/2)^- \to B_Q\pi\pi$.

- $B^*_Q(1/2)^-$: $\mathscr{M}_2(\tilde{B}^*_Q)$ and $\mathscr{M}_4(\tilde{B}^{*\prime}_Q)$ are suppressed by $D-$**wave** decay.

- $B^*_Q(3/2)^-$: $\mathscr{M}_2(\tilde{B}^*_Q)$ and $\mathscr{M}_4(\tilde{B}^{*\prime}_Q)$ are expected to be dominated by $S-$**wave** decay.

- The total amplitude is a coherent sum of the amplitudes given by →

$$\mathscr{T}_{\text{total}} = \sum_{i=1}^{5} \mathscr{T}_i \tag{6}$$

- The three-body decay width →

$$\Gamma = \frac{1}{32M^3(2\pi)^3} \int |\bar{\mathscr{T}}|^2 \mathrm{d}m^2_{\pi_1\pi_2} \mathrm{d}m^2_{\pi_2 B_Q} \tag{7}$$

Methodology

Coupling constants

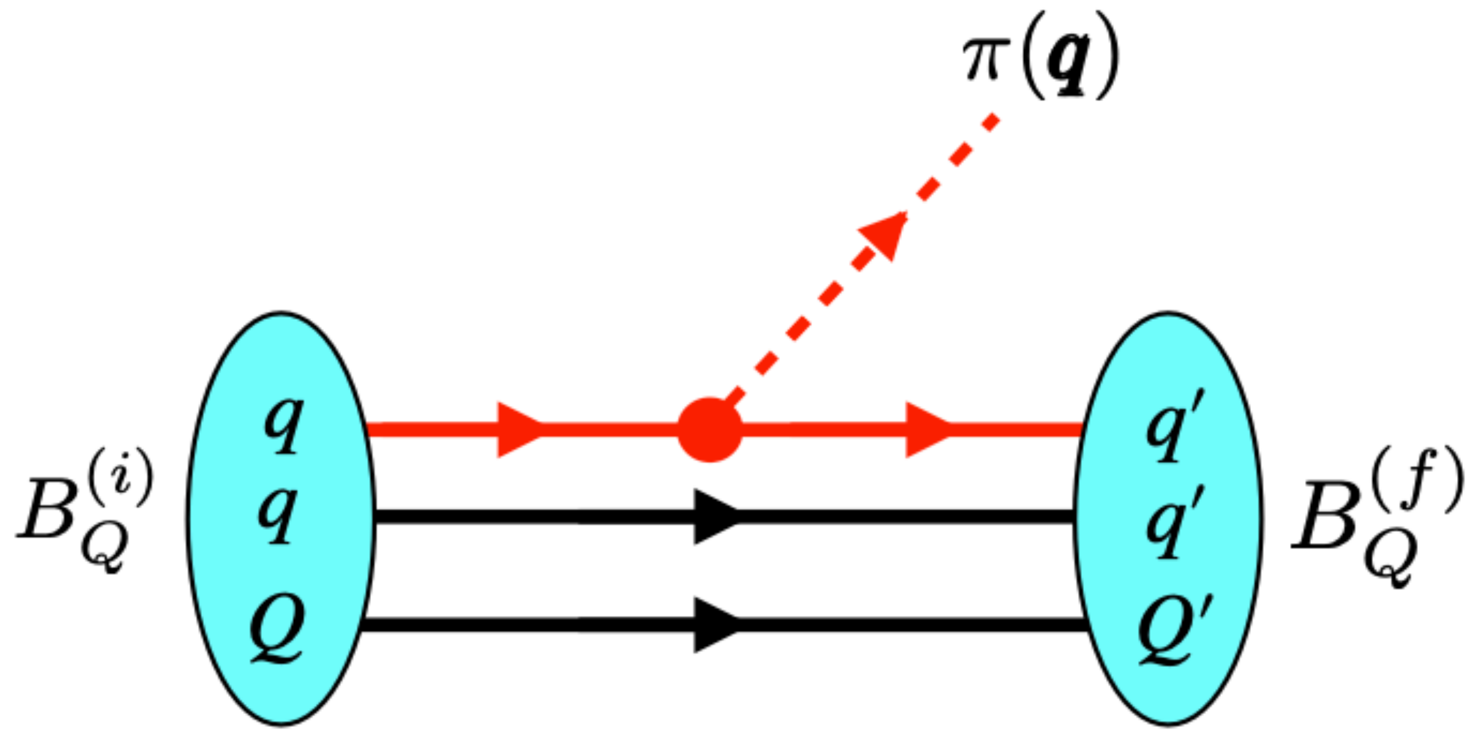

Fig.2 One-pion emission decays of heavy baryons in the quark model.

- **Chiral Quark Model:** Explain the use of the chiral quark model in calculating coupling constants for sequential processes in the two-pion emission decays.
- **Chiral-Partner Structure:** Describe the chiral-partner scheme for estimating the direct process couplings and its importance in understanding decay asymmetry[1].

$$\mathscr{L}_{\pi qq} = \frac{g_A^q}{2_\pi} \bar{q}\gamma_\mu\gamma_5 \boldsymbol{\tau} q \cdot \partial^\mu \boldsymbol{\pi} \tag{8}$$

Non-relativistic

$$\mathscr{H}_{\pi qq} = \frac{g_A^q}{2f_\pi}\left[\boldsymbol{\sigma} \cdot \boldsymbol{q_\pi} + \frac{E_\pi}{2m_q}(\boldsymbol{\sigma} \cdot \boldsymbol{q_\pi} - 2\boldsymbol{\sigma} \cdot \boldsymbol{p_i})\right] \tag{9}$$

Coupling constants

- Decay amplitudes, expressed as helicity amplitudes A_h, are computed by sandwiching $H_{\pi qq}$ between the initial and final states of heavy baryon wave functions

- For $P-$wave decay of $\tilde{B}_Q^{(*)} \to B_Q\pi$ the helicity amplitude, A_h are given by [1]

$$-iA_{1/2} = q\mathcal{O}_1 c_1 \tau, \qquad (10)$$

- The helicity amplitude of $B_Q^*(J^-) \to \tilde{B}_Q^{(*)}\pi$ are given by [1]

$$-iA_h = (\mathcal{O}_0^\lambda c_0 + q^2\mathcal{O}_2^\lambda c_2)\tau \,. \qquad (11)$$

where

$$\mathcal{O}_1 = G_a\left(2 + \frac{\omega}{2m_q + m_Q}\right)F(q^2),$$

$$G_a = \frac{g_A^q}{2f_\pi}\sqrt{2M_{B_Q}}$$

$$F(q^2) = \mathrm{e}^{-q_\lambda^2/4a_\lambda^2}\mathrm{e}^{-q_\rho^2/4a_\rho^2},$$

$$\mathcal{O}_0^\lambda = \frac{iG_b a_\lambda \omega}{m_q}F(q^2),$$

$$\mathcal{O}_2^\lambda = \frac{iG_b m_Q}{a_\lambda(2m_q + m_Q)}\left(2 + \frac{\omega}{2m_q + m_Q}\right)F(q^2),$$

$$G_b = \frac{g_A^q}{2f_\pi}\sqrt{2M_{B_Q^*}}\sqrt{2M_{\tilde{B}_Q^{(*)}}}\,.$$

Numerical results

Dalitz boundaries and resonance bands

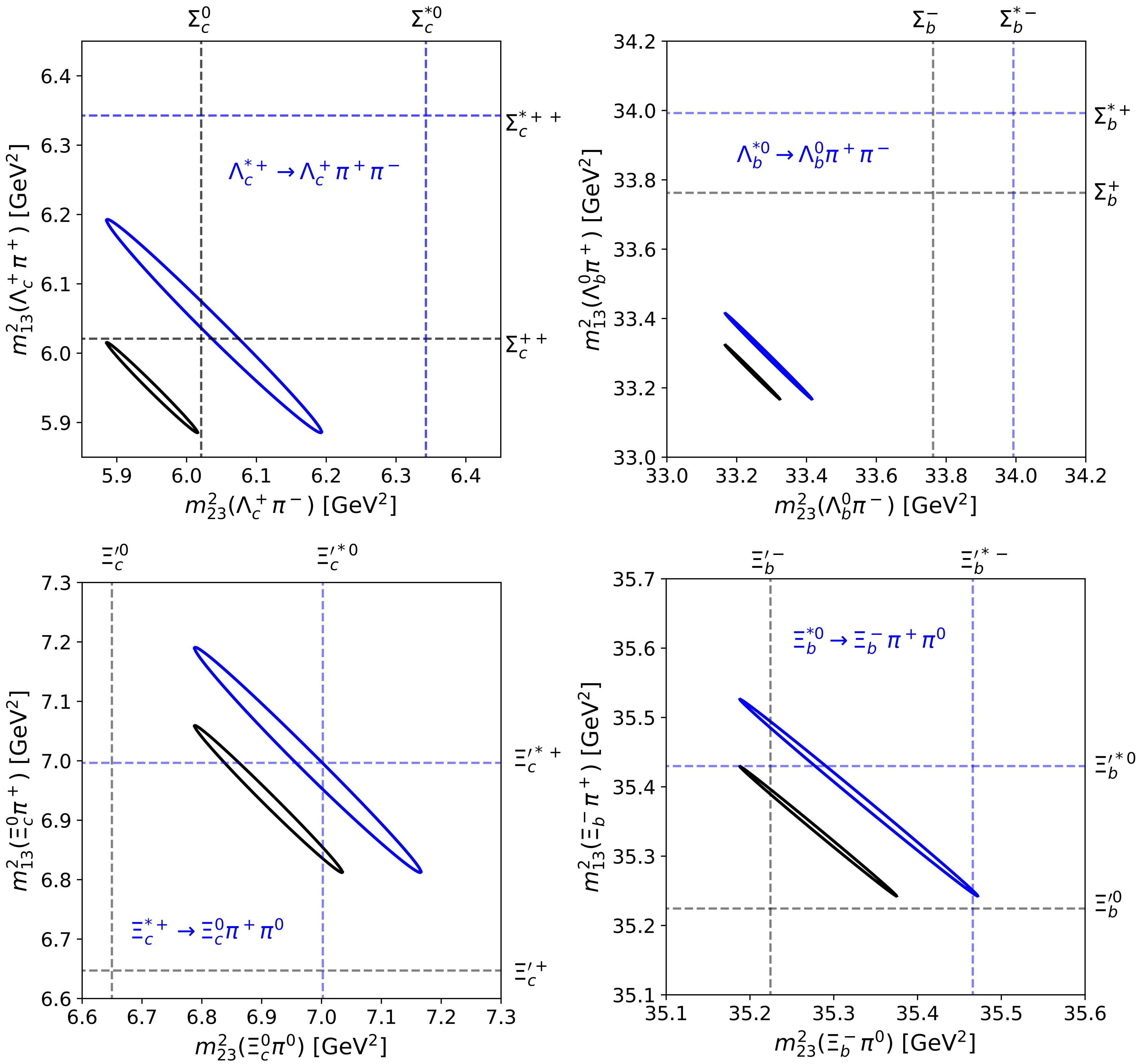

Fig.3 The Dalitz boundary for two pion emission decays.

- $B_Q^*(1/2^-) \to \tilde{B}_Q(1/2^+)\pi \quad S-$wave,

  $\to \tilde{B}_Q(3/2^+)\pi \quad D-$Wave,

- $B_Q^*(3/2^-) \to \tilde{B}_Q(1/2^+)\pi \quad D-$wave,

  $\to \tilde{B}_Q(3/2^+)\pi \quad S-$Wave,

- The $\Sigma_c(1/2^+)$ with $S-$wave resides near the boundary for $\Lambda_c^*(1/2)$, while the $\Lambda_c^*(3/2^-)$ is well within the plots.
- The $\Sigma_c^*(3/2^-)$ is outside the plots.
- For $\Lambda_b(1/2^-)$ and $\Lambda_b(3/2^-)$, the $\Sigma_b^{(*)}$ resonance bands are outside the plot and appear non-resonant inside the Dalitz plot.

$\Lambda_c(2595)^+$

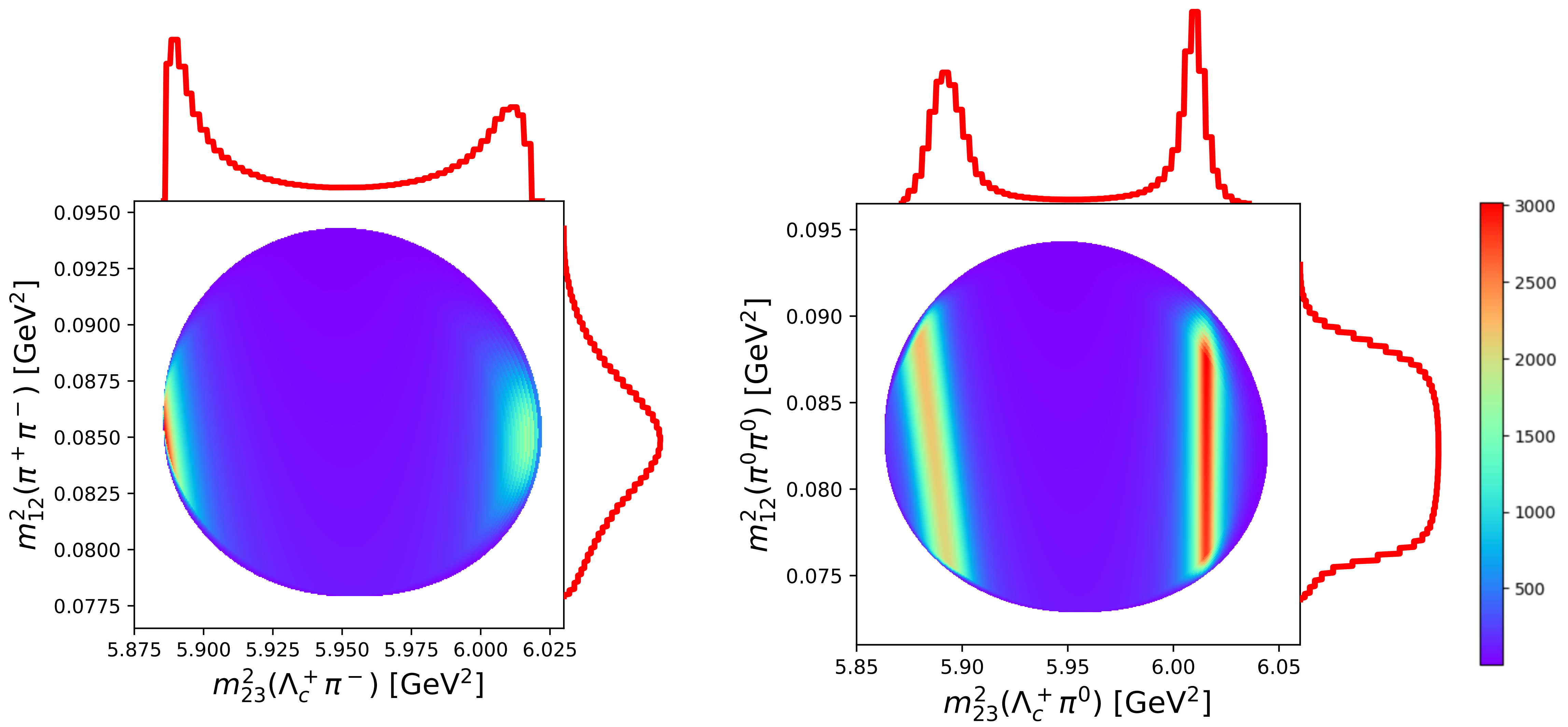

Fig.3 Dalitz plots and invariant mass distribution of $\Lambda_c(2595)$ as $1/2^-$ with $\lambda-$mode in the quark model to (a) $\Lambda_c\pi^+\pi^-$ and (b) $\Lambda_c\pi^0\pi^0$.

- The decay of $\Lambda_c(2595)$ is also know to exhibit a large isospin symmetry breaking.

$$R = \frac{\mathscr{B}(\Lambda_c^+\pi^+\pi^-)}{\mathscr{B}(\Lambda_c^+\pi^0\pi^0)} \approx 4$$

Our calculation → 3.85

Table 1 The total and partial decay width of $\Lambda_c^+(2595)$ and $\Lambda_c^+(2625)$.

Decay mode	$\Lambda_c(2595)^+$		$\Lambda_c(2625)^+$	
	Model	Expt	Model	Expt
(1) $\Lambda_c\pi^+\pi^-$	0.399		0.325	50.7%
$\to \Sigma_c^0\pi^+$	0.182	$0.624(24\pm7\%)$	0.029	5.19%
$\to \Sigma_c^{++}\pi^-$	0.162	$0.624(24\pm7\%)$	0.028	5.13%
$\to \Sigma_c^{*0}\pi^+$	$1.058e-06$		0.043	
$\to \Sigma_c^{*++}\pi^-$	$1.060e-06$		0.044	
$\to$ Direct (3-body)	0.004	$0.468(18\pm10\%)$	0.053	Large
$\to$ Interference	0.054		0.128	
(2) $\Lambda_c\pi^0\pi^0$	1.537		0.245	
$\to \Sigma_c^+\pi^0$	1.494		0.037	
$\to \Sigma_c^{*+}\pi^0$	$4.340e-06$		0.071	
$\to$ Direct (3-body)	0.004		0.039	
$\to$ Interference	0.038		0.098	
Total	1.936	2.6 ± 0.6	0.570	< 0.52

- **We note that the contribution from the Σ_c^* resonance is approximately 10^6 due to its very being close to the threshold.**

$\Lambda_c(2595)^+$

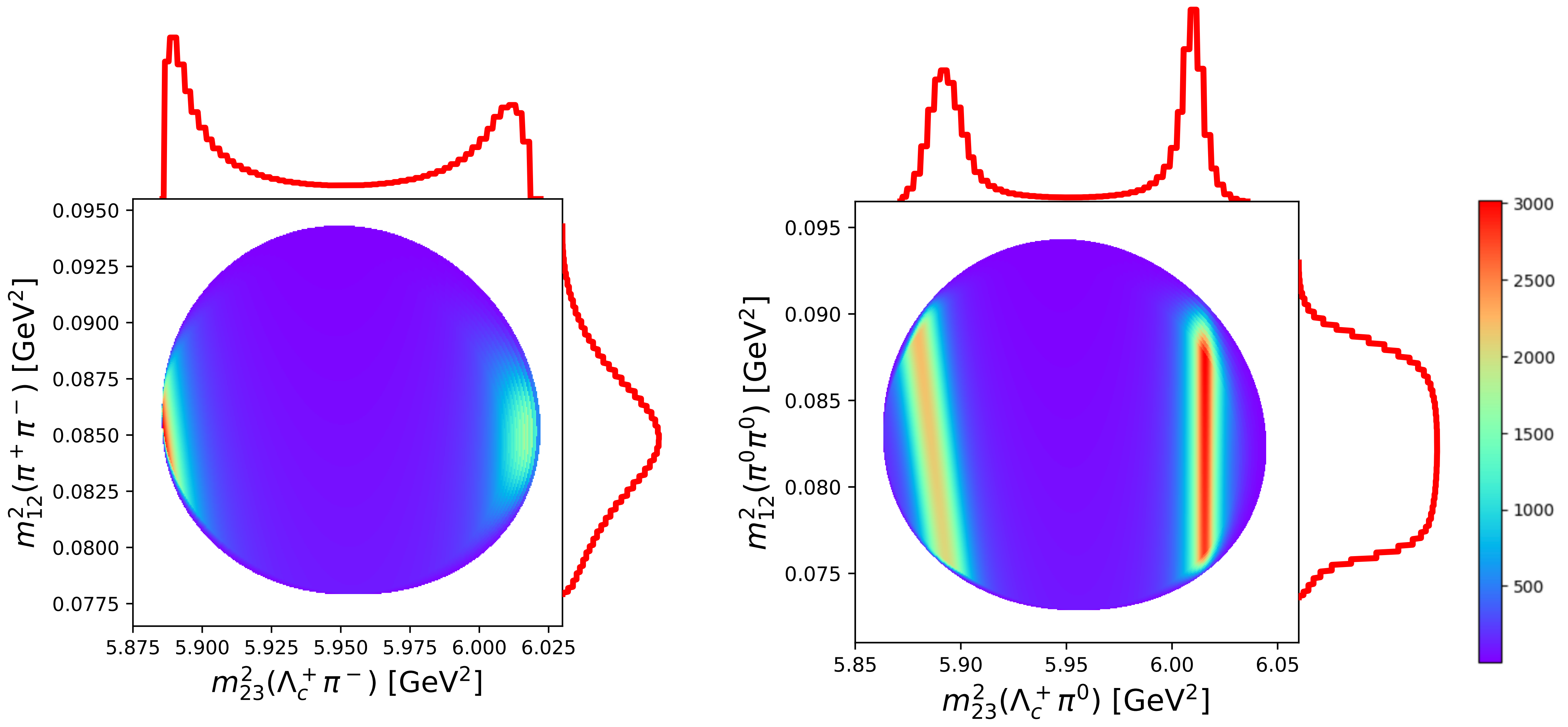

Fig.4 Dalitz plots and invariant mass distribution of $\Lambda_c(2595)$ as $1/2^-$ with $\lambda-$mode in the quark model to (a) $\Lambda_c\pi^+\pi^-$ and (b) $\Lambda_c\pi^0\pi^0$.

- The direct process is small and hindered by the dominant $S-$ wave resonance.
- The width is around $2\ \mathrm{MeV}$ the finite width effect, where the resonance bands near the Dalitz boundary and the kinematical reflection (diagonal bands) are smeared.
- Fig.4 shows some results of the Dalitz plot for $\Lambda_c(2595) \to \Lambda_c^+\pi^+\pi^-$ and $\Lambda_c(2595) \to \Lambda_c^+\pi^0\pi^0$ which different positions of $\Sigma_c(1/2^+)$ resonance bands.
- The convolution is evident in the smearing of the resonance bands near the Dalitz boundary.

$\Lambda_c(2625)^+$

- In Fig.5, we present our calculated Dalitz and invariant mass plots, which agree with those reported by Belle.
- Since the width is small $\Gamma_{exp} < 0.52$ MeV, the smearing effect is relatively small; it only enlarges the plot as seen near the boundary.
- Our calculation $\Gamma_{our} = 0.570$ MeV.
- In the upper and right sides of the Dalitz plot, we compare the structure of the $\Lambda_c^+\pi^+$ and $\pi^+\pi^-$ invariant mass distributions with recent Belle data.[2].
- Note that this is a simple comparison with the data, which was not obtained by the fit.
- The coupling constants are computed from the quark model [1], and the ratio of the couplings is essential in determining the structure in an invariant mass plot.

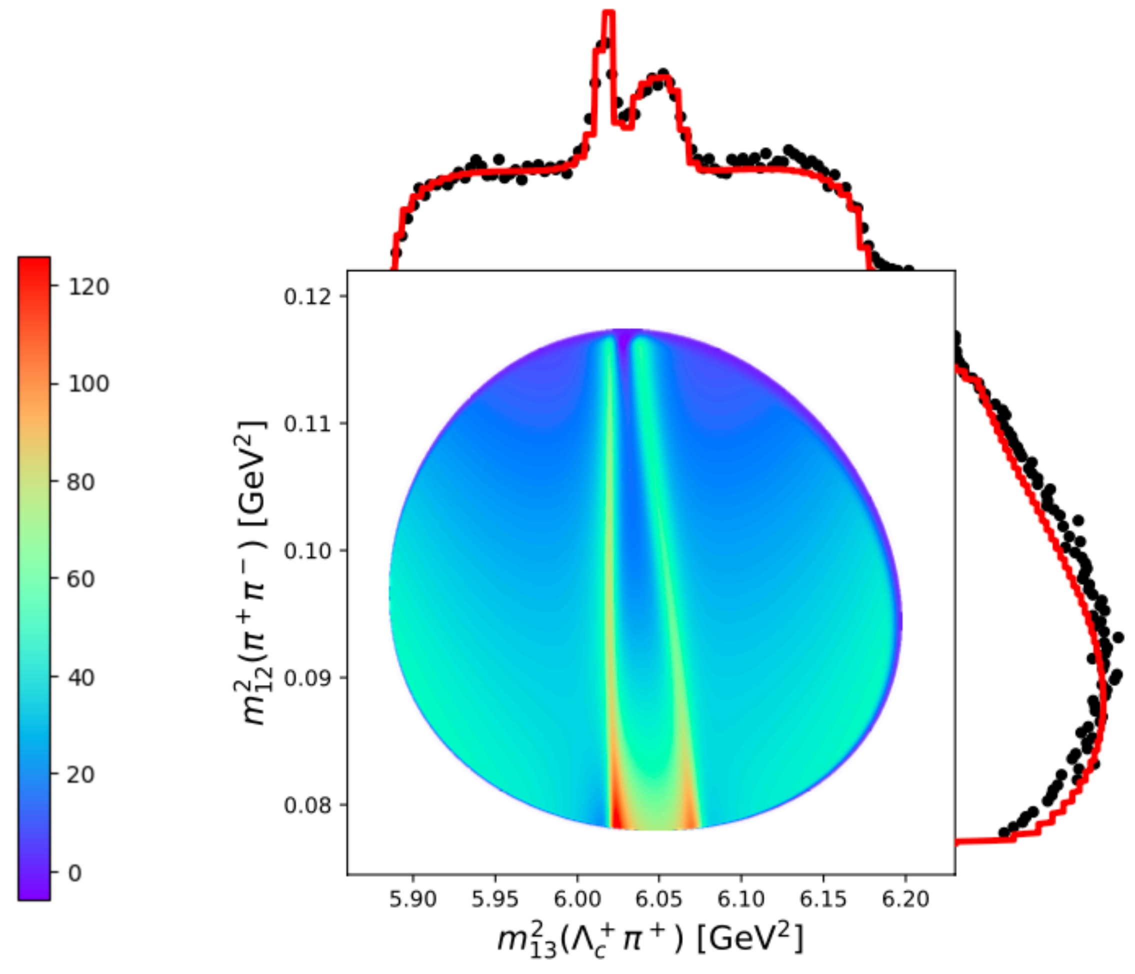

Fig.5 Dalitz plots and invariant mass distribution of $\Lambda_c(2625)$as $3/2^-$with $\lambda-$mode in the quark model.

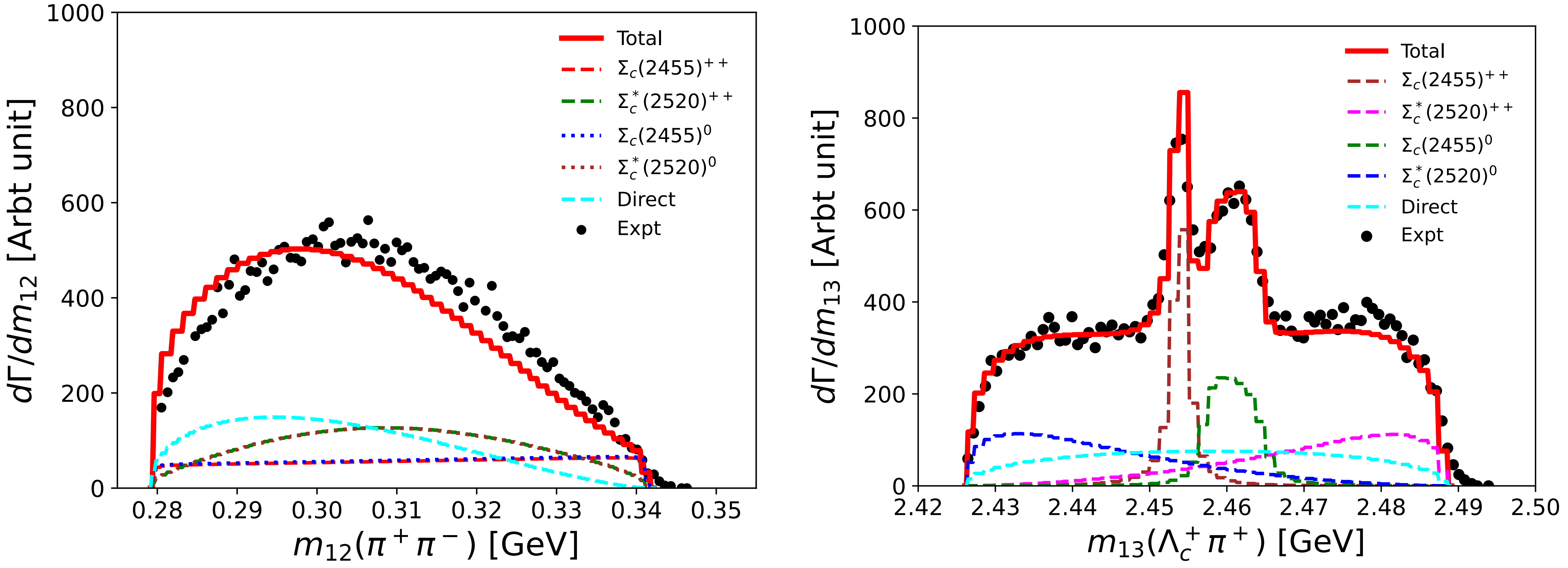

Fig.6 The $\Lambda_c^+\pi^+$ and $\pi^+\pi^-$ invariant mass plot of $\Lambda_c(2625)^+$

$\Lambda_c(2625)^+$

We can also express the ratio as follows.

$$R_1 = \frac{\mathcal{B}(\Lambda_c(2625)^+ \to \Sigma_c^0 \pi^+)}{\mathcal{B}(\Lambda_c(2625)^+ \to \Lambda_c^+ \pi^+ \pi^-)} = 5.19 \pm 0.23\,\%\,,$$

$$R_2 = \frac{\mathcal{B}(\Lambda_c(2625)^+ \to \Sigma_c^{++} \pi^-)}{\mathcal{B}(\Lambda_c(2625)^+ \to \Lambda_c^+ \pi^+ \pi^-)} = 5.13 \pm 0.26\,\%\,,$$

Our results have values of $R_1 = 8.92\,\%$ and $R_2 = 8.61\,\%$

Which are ***slightly larger than the surrounding data.***

- Form Dalitz plot, we found that the effect of the convolution is rather small.
- We compared the shape of the invariant mass distribution $m^2_{\Lambda_c^+\pi^+}$ and $m^2_{m_{\pi^+}m_{\pi^-}}$ with recent Belle data
- The contributions of $\Sigma_c(1/2^+)$ is larger than the Belle data.
- It is related to the branching ratio R_1 and R_2.

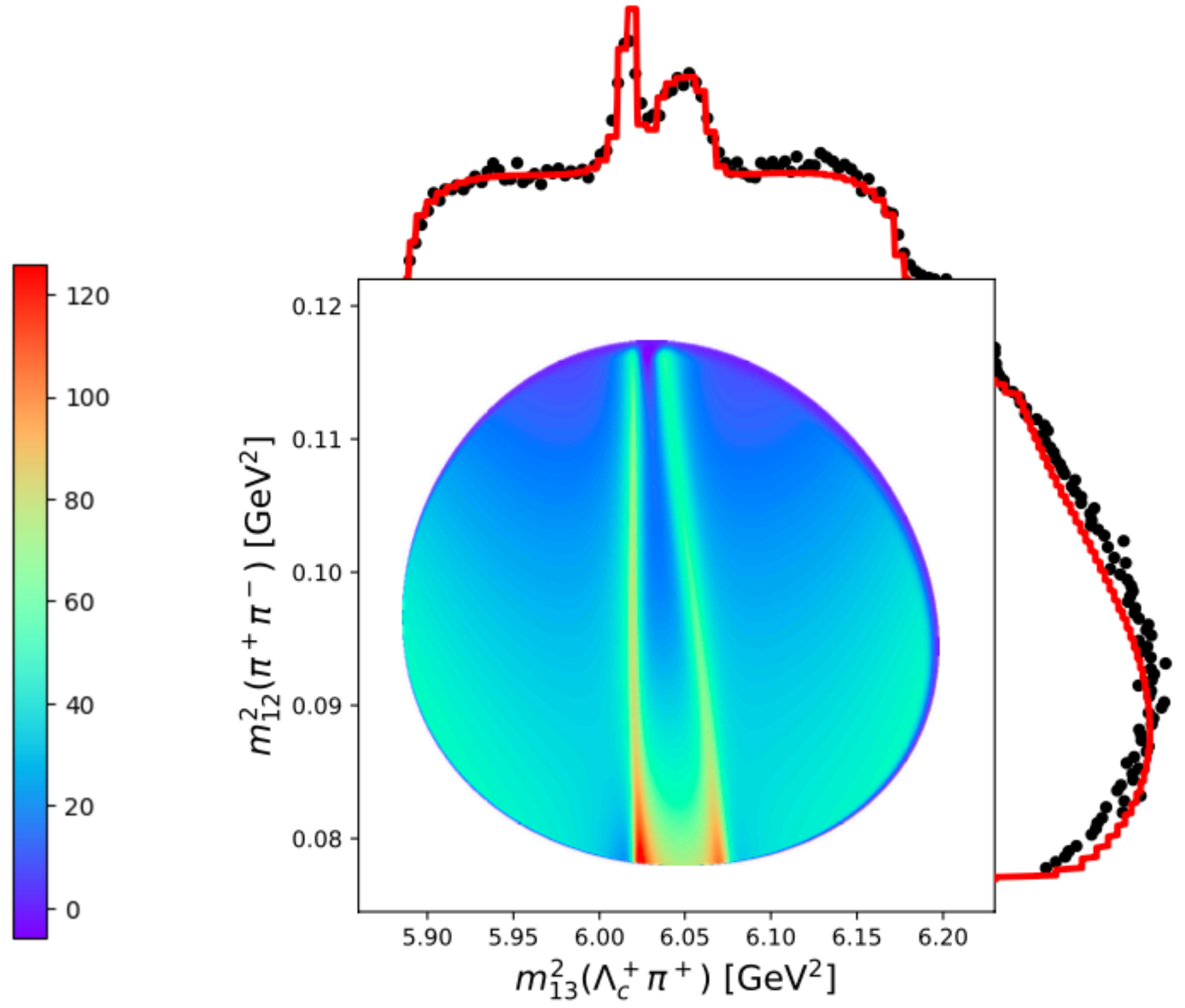

$\Lambda_b(5912)^0$

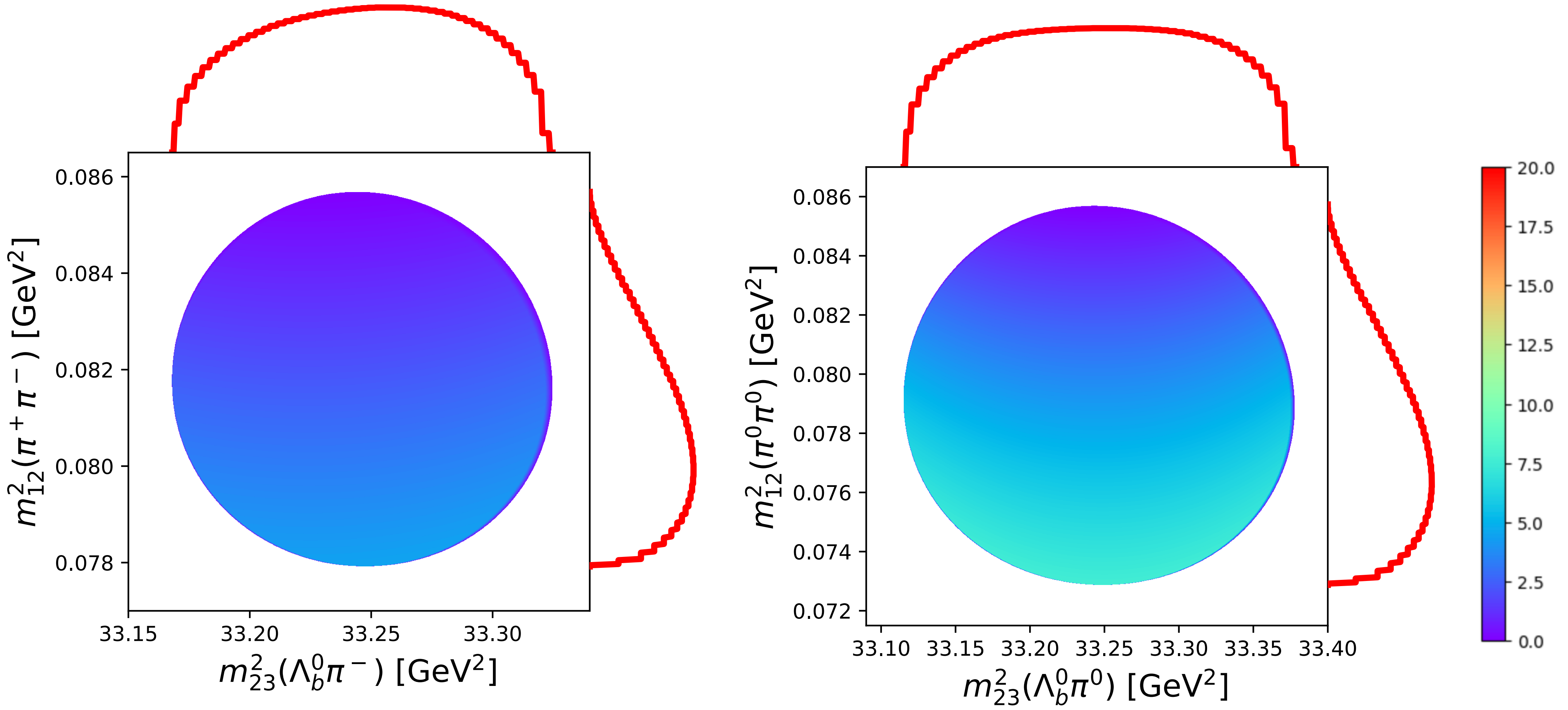

Fig. 7 Dalitz plots and invariant mass distribution of $\Lambda_b(5912)$as $1/2^-$with $\lambda-$mode in the quark model to (a) $\Lambda_b\pi^+\pi^-$and (b) $\Lambda_b\pi^0\pi^0$.

- In the quark model, the calculated decay width with the $\lambda-$mode is consistent with the upper limit of the experimental data, as shown in Table 3.
- We observe that the direct process is significant partly because the $\Sigma_b\pi$ decay is unopened and, thus, is suppressed.
- Since it is closed, the $\Sigma_b^{(*)}$ resonance will not be visible as a resonance band on the Dalitz plot.

Table 3. The total and partial decay width of $\Lambda_b^0(5912)$ and $\Lambda_b^0(5920)$.

Decay mode	$\Lambda_b(5912)^0$		$\Lambda_b(5920)^0$	
	Model	Expt	Model	Expt
(1) $\Lambda_b\pi^+\pi^-$	0.0031		0.009	
$\to \Sigma_b^-\pi^+$	0.0005		$7.907e-07$	
$\to \Sigma_b^+\pi^-$	0.0006		$9.960e-07$	
$\to \Sigma_b^{*-}\pi^+$	$6.846e-8$		0.001	
$\to \Sigma_b^{*+}\pi^-$	$7.764e-8$		0.001	
$\to$ Direct (3-body)	0.0005		0.002	
$\to$ Interference	0.0015		0.005	
(2) $\Lambda_b\pi^0\pi^0$	0.0077		0.013	
$\to \Sigma_b^0\pi^0$	0.0028		$4.376e-06$	
$\to \Sigma_b^{*0}\pi^0$	$9.608e-07$		0.003	
$\to$ Direct (3-body)	0.0012		0.003	
$\to$ Interference	0.0036		0.007	
Total	0.0108	< 0.25	0.022	< 0.19

$\Lambda_b(5920)^0$

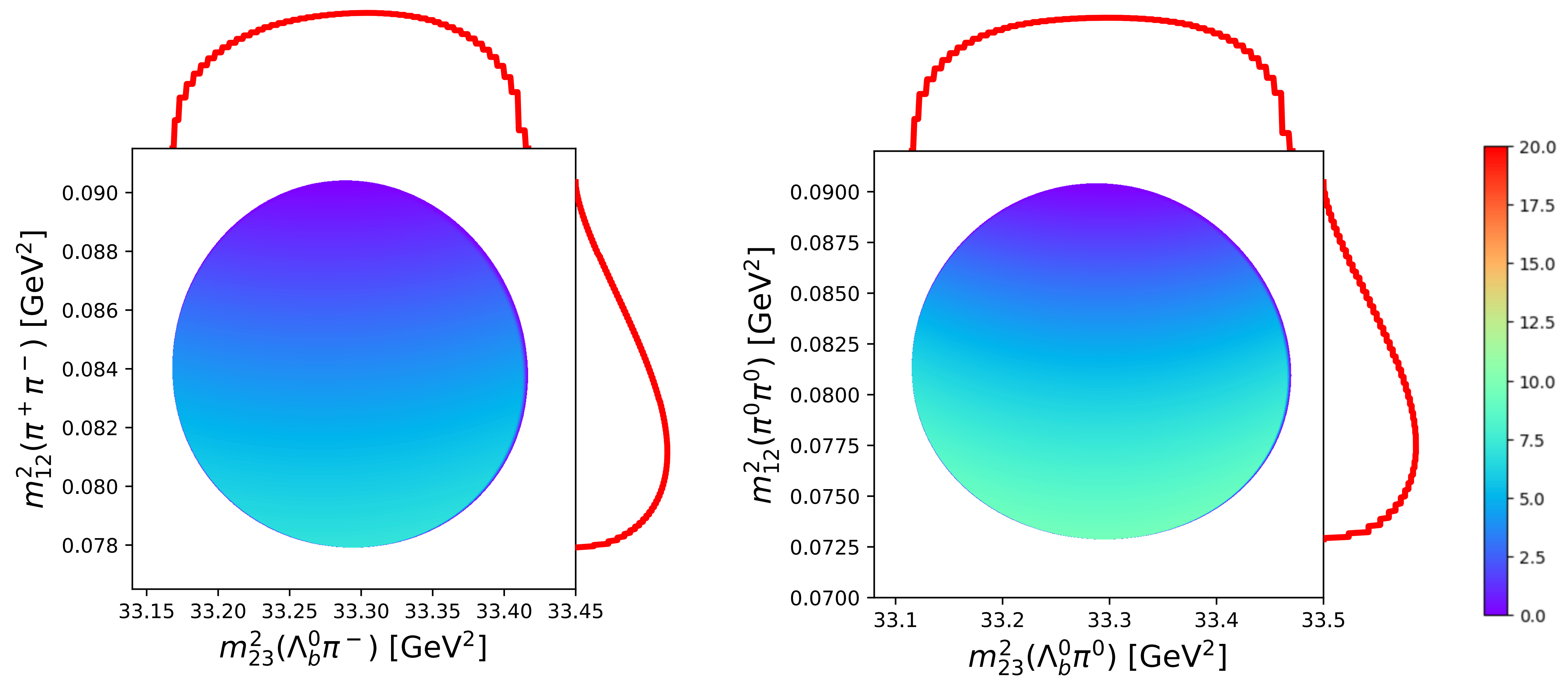

Fig. 8 Dalitz plots and invariant mass distribution of $\Lambda_b(5920)$as $1/2^-$with $\lambda-$mode in the quark model to (a) $\Lambda_b\pi^+\pi^-$and (b) $\Lambda_b\pi^0\pi^0$.

- The $\Lambda_b^0(5920)$ baryon is expected to be very narrow and have a spin of $J^P = 3/2^-$.
- The upper limit of the decay width is $\Gamma_{exp} < 0.19$ MeV.
- The decays into $\Lambda_b\pi\pi$, with the non-resonant process contributing significantly to this decays.
- The threshold for $\Sigma_b^{(*)}$ decay is closed.
- The two-body decays of $\Lambda_b^*(5920)$ into $\Sigma_b^{(*)}$ are closed.
- Since it is closed, the $\Sigma_b^{(*)}$ resonance will not be visible as a resonance band on the Dalitz plot.
- The $\pi^+\pi^-$ invariant mass distribution has an asymmetric pattern.
- The invariant mass distribution of $\pi^+\pi^-$ is more pronounced towards the lower side.

$\Lambda_b(5920)^0$

- The calculated decay width is consistent with the upper limit of the experimental data.
- We note that the non-resonant contribution is significant in this process.
- The finite contribution of the non-resonant contribution is due to the chiral partner structure.
- The coupling strength of the direct process is equivalent to the vertex in the three-body decay.

Table 3. The total and partial decay width of $\Lambda_b^0(5912)$ and $\Lambda_b^0(5920)$.

Decay mode	$\Lambda_b(5912)^0$		$\Lambda_b(5920)^0$	
	Model	Expt	Model	Expt
(1) $\Lambda_b\pi^+\pi^-$	0.0031		0.009	
$\to \Sigma_b^-\pi^+$	0.0005		$7.907e-07$	
$\to \Sigma_b^+\pi^-$	0.0006		$9.960e-07$	
$\to \Sigma_b^{*-}\pi^+$	$6.846e-8$		0.001	
$\to \Sigma_b^{*+}\pi^-$	$7.764e-8$		0.001	
$\to$ Direct (3-body)	0.0005		0.002	
$\to$ Interference	0.0015		0.005	
(2) $\Lambda_b\pi^0\pi^0$	0.0077		0.013	
$\to \Sigma_b^0\pi^0$	0.0028		$4.376e-06$	
$\to \Sigma_b^{*0}\pi^0$	$9.608e-07$		0.003	
$\to$ Direct (3-body)	0.0012		0.003	
$\to$ Interference	0.0036		0.007	
Total	0.0108	< 0.25	0.022	< 0.19

$\Xi_c(2790)^+$

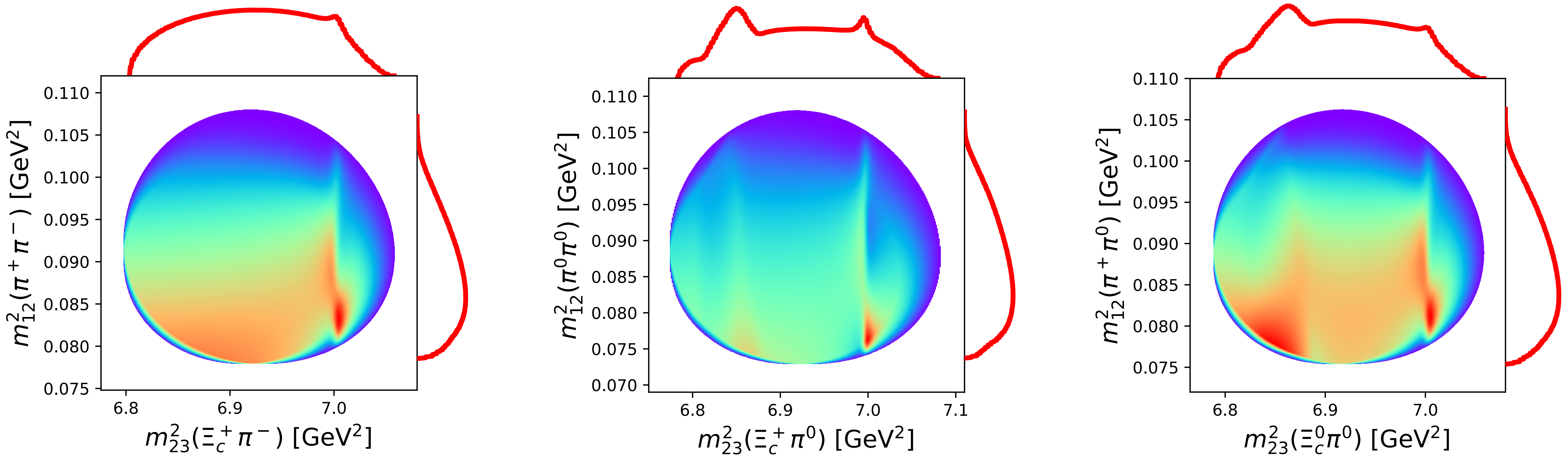

- The $\Xi_c(2790)^+$ was observed in $\Xi_c^{P\prime}(1/2^+)\pi$ and $\Xi_c\gamma$ with a total width of 8.9 ± 1.0 MeV.
- In PDG, $\Xi_c(2790)^+$ it is assigned as a $1/2^-$ state from the quark model expectation, although the spin-parity has not been directly measured.
- The decay $\Xi_c(2790)^+$ is consistent with the $1/2$ and $\lambda-$ mode.

Table 4. Total and partial decay widths of $\Xi_c(2780)^+$ and $\Xi_c(2815)^+$ decays, the widths are given in units of MeV, and a comparison with experimental data is also presented.

Decay mode	$\Xi_c(2790)^+$		$\Xi_c(2815)^+$	
	Our	Expt.	Our	Expt.
(1) $\Xi_c^{\prime +}\pi^0$	2.3367		0.118	
(2) $\Xi_c^{\prime 0}\pi^+$	4.6244		0.215	
(3) $\Xi_c^+\pi^-\pi^+$	0.0101		1.460	
$\to \Xi_c^{\prime *0}\pi^+$	0.0002		1.453	
$\to$ Direct (3-body)	0.0098		0.038	
$\to$ Interference	0.0001		-0.031	
(4) $\Xi_c^+\pi^0\pi^0$	0.0045		0.472	
$\to \Xi_c^{\prime *+}\pi^0$	0.0003		0.475	
$\to$ Direct (3-body)	0.0041		0.014	
$\to$ Interference	0.0001		-0.016	
(5) $\Xi_c^0\pi^+\pi^0$	0.0114		1.856	
$\to \Xi_c^{\prime *+}\pi^0$	0.0002		0.363	
$\to \Xi_c^{\prime *0}\pi^+$	0.0003		1.507	
$\to$ Direct (3-body)	0.0108		0.041	
$\to$ Interference	0.0002		-0.055	
Total	6.9871	8.9 ± 1.0	4.121	2.43 ± 0.26

$\Xi_c(2815)^+$

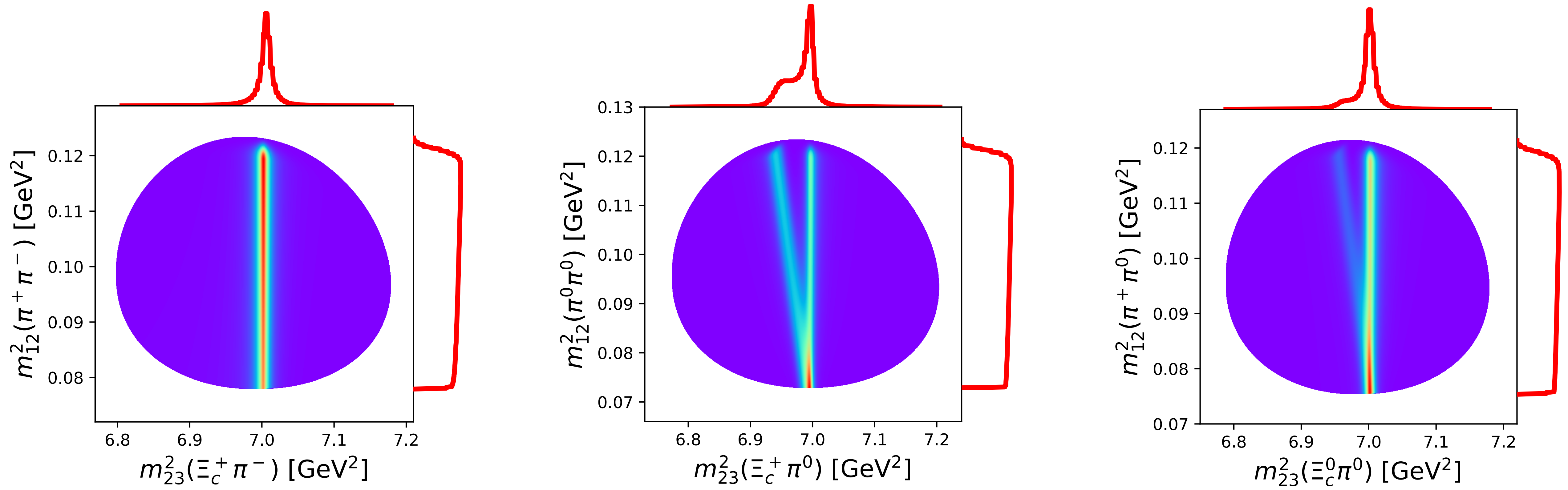

- The decay occurs in a $S-$wave.
- The Dalitz plots show a pronounced $\Xi_c'(2645)$ resonance band with a very small nonresonant contribution.
- The decays are fascinating because the Dalitz plot shows distinct cross-diagram structures, appearing as diagonal bands.
- It should be noted that the direct coupling process is fixed according to the chiral-partner scheme.[3],[4]

Table 5. Total and partial decay widths of $\Xi_c(2780)^+$ and $\Xi_c(2815)^+$ decays, the widths are given in units of MeV, and a comparison with experimental data is also presented.

Decay mode	$\Xi_c(2790)^+$		$\Xi_c(2815)^+$	
	Our	Expt.	Our	Expt.
(1) $\Xi_c'^+\pi^0$	2.3367		0.118	
(2) $\Xi_c'^0\pi^+$	4.6244		0.215	
(3) $\Xi_c^+\pi^-\pi^+$	0.0101		1.460	
$\to \Xi_c'^{*0}\pi^+$	0.0002		1.453	
$\to$ Direct (3-body)	0.0098		0.038	
$\to$ Interference	0.0001		-0.031	
(4) $\Xi_c^+\pi^0\pi^0$	0.0045		0.472	
$\to \Xi_c'^{*+}\pi^0$	0.0003		0.475	
$\to$ Direct (3-body)	0.0041		0.014	
$\to$ Interference	0.0001		-0.016	
(5) $\Xi_c^0\pi^+\pi^0$	0.0114		1.856	
$\to \Xi_c'^{*+}\pi^0$	0.0002		0.363	
$\to \Xi_c'^{*0}\pi^+$	0.0003		1.507	
$\to$ Direct (3-body)	0.0108		0.041	
$\to$ Interference	0.0002		-0.055	
Total	6.9871	8.9 ± 1.0	4.121	2.43 ± 0.26

$\Xi_b(6087)^0$

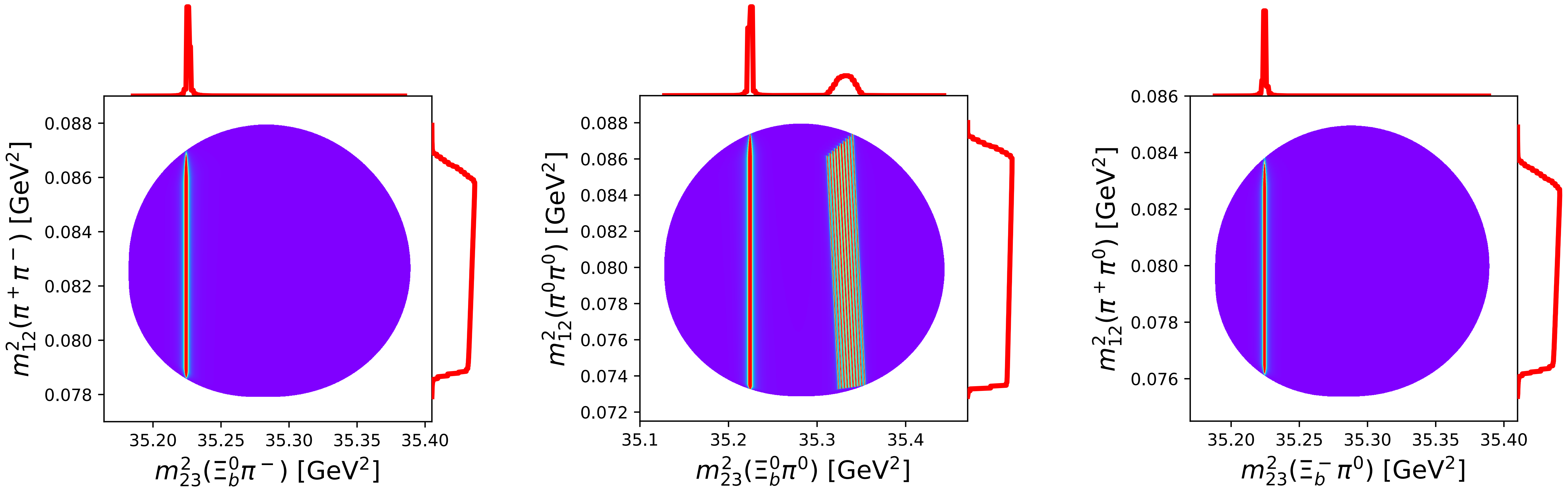

Table 6. Total and partial decay widths of $\Xi_b(6087)^0$ and $\Xi_b(6095)^0$ decays, the widths are given in units of MeV, and a comparison with experimental data is also presented.

Decay mode	$\Xi_b(6087)^0$ Our	$\Xi_b(6087)^0$ Expt.	$\Xi_b(6095)^0$ Our	$\Xi_b(6095)^0$ Expt.
(1) $\Xi_b^0\pi^-\pi^+$	0.7440		0.1200	
$\to \Xi_b'^-\pi^+$	0.7467		0.0024	
$\to \Xi_b'^{*-}\pi^+$	... [a]		0.1056	
$\to$ Direct (3-body)	0.0005		0.0016	
$\to$ Interference	-0.0032		0.0103	
(2) $\Xi_b^0\pi^0\pi^0$	0.7070		0.2312	
$\to \Xi_b'^0\pi^0$	0.7092		0.0032	
$\to \Xi_b'^{*0}\pi^0$	... [a]		0.2252	
$\to$ Direct (3-body)	0.0004		0.0010	
$\to$ Interference	-0.0027		0.0017	
(3) $\Xi_b^-\pi^+\pi^0$	0.5623		0.2189	
$\to \Xi_b'^0\pi^0$	0.0008		... [a]	
$\to \Xi_b'^-\pi^+$	0.5648		0.0018	
$\to \Xi_b'^{*0}\pi^0$	... [a]		0.1095	
$\to \Xi_b'^{*-}\pi^+$	... [a]		0.0973	
$\to$ Direct (3-body)	0.0004		0.0015	
$\to$ Interference	-0.0037		0.0088	
Total	2.0133	2.43 ± 0.51	0.5701	0.50 ± 0.33

- This $\Xi_b(6087)^0$ was recently discovered by LHCb [5].
- The measured width of $2.4 \pm 0.51 \pm 0.10$ MeV is consistent with a $1/2^-$state with a $\lambda-$mode, as shown in Table 6.
- The two-pion emission decay is primarily dominated by the Ξ_b' intermediate state.
- The decay via the $\Xi_b^{*\prime}$intermediate state is negligible since it occurs virtually and through a $D-$wave.

$\Xi_b(6095)^0$

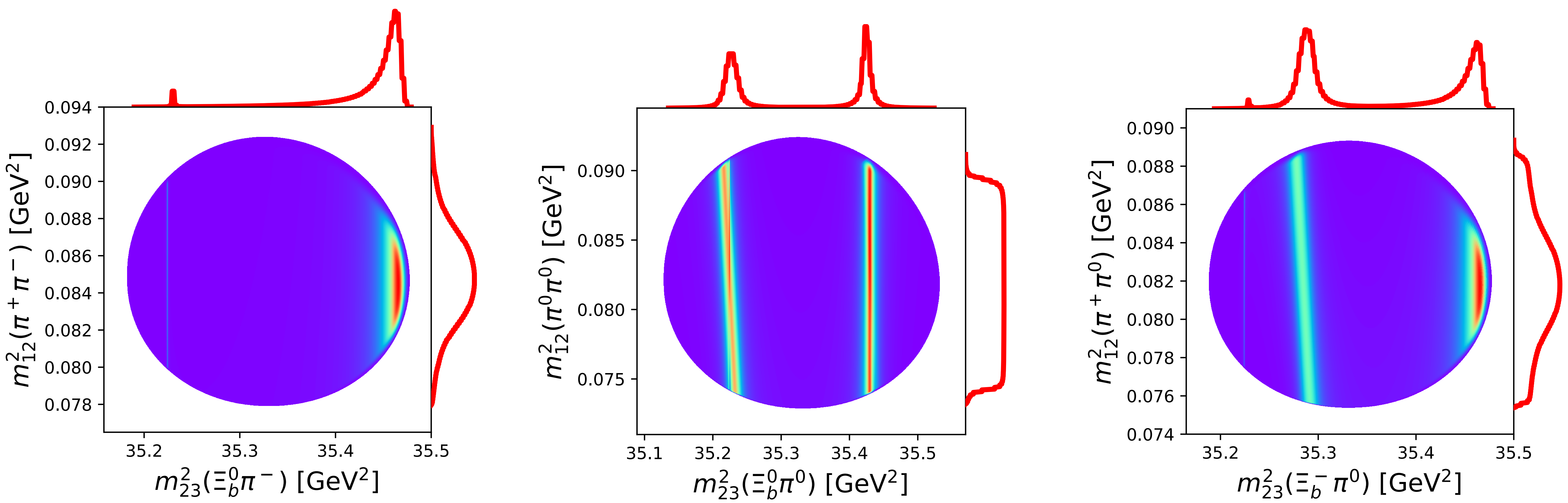

- This $\Xi_b(6090)^0$ was recently discovered by LHCb [4] via the $\Xi_b^{*\prime -}(\Xi_b^0\pi^-)\pi^+$ decay and is possibly an isospin partner of Ξb(6100) found earlier by CMS.
- The measured width of 0.50 MeV agrees with a $3/2^-$state with a $\lambda-$mode excitation, as shown in Table 7.
- The decay is dominated by the $S-$wave $\Xi_b^{*\prime}\pi$ mode, which subsequently decays into $\Xi_b\pi\pi$

Table7. Total and partial decay widths of $\Xi_b(6087)^0$ and $\Xi_b(6095)^0$ decays, the widths are given in units of MeV, and a comparison with experimental data is also presented.

Decay mode	$\Xi_b(6087)^0$		$\Xi_b(6095)^0$	
	Our	Expt.	Our	Expt.
(1) $\Xi_b^0\pi^-\pi^+$	0.7440		0.1200	
$\to \Xi_b^{\prime -}\pi^+$	0.7467		0.0024	
$\to \Xi_b^{\prime *-}\pi^+$	... [a]		0.1056	
$\to$ Direct (3-body)	0.0005		0.0016	
$\to$ Interference	-0.0032		0.0103	
(2) $\Xi_b^0\pi^0\pi^0$	0.7070		0.2312	
$\to \Xi_b^{\prime 0}\pi^0$	0.7092		0.0032	
$\to \Xi_b^{\prime *0}\pi^0$	... [a]		0.2252	
$\to$ Direct (3-body)	0.0004		0.0010	
$\to$ Interference	-0.0027		0.0017	
(3) $\Xi_b^-\pi^+\pi^0$	0.5623		0.2189	
$\to \Xi_b^{\prime 0}\pi^0$	0.0008		... [a]	
$\to \Xi_b^{\prime -}\pi^+$	0.5648		0.0018	
$\to \Xi_b^{\prime *0}\pi^0$	... [a]		0.1095	
$\to \Xi_b^{\prime *-}\pi^+$	... [a]		0.0973	
$\to$ Direct (3-body)	0.0004		0.0015	
$\to$ Interference	-0.0037		0.0088	
Total	2.0133	2.43 ± 0.51	0.5701	0.50 ± 0.33

Conclusion

- We have analyzed the two-pion emissions decays of the singly heavy baryons of Λ_Q and Ξ_Q with $J^p = 1/2$ and $J^p = 3/2$.
- We consider both sequential processes through intermediate states of the symmetric flavor sextet 6_F, $\Sigma_Q$and Ξ'_Q, with $j^p = 1/2+$ and $3/2^+$.
- The direct two-pion process is also included, which is essential for comparison with experimental data.
- The coupling for the sequential process is derived from the chiral quark model, while the direct process is assumed to follow the chiral partner scheme.
- The convolution of the initial parent's mass for the Dalitz plot is also considered to obtain a more realistic comparison with the data.

Conclusion

- Our decay analysis, compared with the available experimental data, further supports the conclusion that these resonances are consistent with a heavy quark symmetry (HQS) doublet with $(1/2^-, 3/2^-)$a brown-muck spin $j = 1$ in the $\lambda-$mode excitation.

- We analysis of the Dalitz and invariant mass plots.

- For the$\Lambda_c(2625)^+$ and found a good description of the Dalitz plot and the $\pi^+\pi^-$ invariant mass distribution.

- We also compared our results with some LHCb data for the $\Lambda_b(5920^0$ decay; however, more data is needed to confirm the observed asymmetry.

- The direct process is suppressed for decays involving baryons when the $S-$wave resonance contributes.

- The contribution of this nonresonant process predicted by the chiral-partner structure in heavy baryon sectors may provide further tests that can be verified in experiments.

- Additionally, the $\Xi_b(6087)^0$and $\Xi_b(6095)^0$ decays may exhibit an isospin-breaking effect similar to that observed in the $\Lambda_c(2595)^+$.

Reference

[1] H. Nagahiro, S. Yasui, A. Hosaka, M. Oka, and H. Noumi, Structure of charmed baryons studied by pionic decays, Phys. Rev. D 95, 014023 (2017).

[2] D. Wang et al. (Belle), Measurement of the mass and width of the $\Lambda_c(2625)^+$charmed baryon and the branching ratios of $\Lambda_c(2625)^+ \to \Xi_c^0\pi^+$and $\Lambda_c(2625)^+ \to \Xi^{++}\pi^-$, Phys. Rev. D 107, 032008 (2023).

[3] R. Aaij et al. (LHCb), Observation of new baryons in the $\Xi_b^-\pi^+\pi^-$ and $\Xi_b^0\pi^+\pi^-$ systems, Phys. Rev. Lett. 131, 171901 (2023).

[3] B Y. Kawakami and M. Harada, Analysis of $\Lambda_c(2595), \Lambda_(2625), \Lambda_b(5912), \Lambda_b(5920)$ based on a chiral partner structure, Phys. Rev. D 97, 114024 (2018).

[4] Y. Kawakami and M. Harada, Singly heavy baryons with chiral partner structure in a three-flavor chiral model, Phys. Rev. D 99, 094016 (2019).

[5] R. Aaij et al. (LHCb), Observation of new baryons in the $\Xi_b^-\pi^+\pi^{--}$ and $\Xi_b^0\pi^+\pi^-$systems, Phys. Rev. Lett. 131, 171901 (2023).